Performance of Permeable Pavement over a Tight, Clay Soil in Durham, North Carolina: Hydrology, Water Quality and the Calibration and Validation of DRAINMOD

Piney Wood Park
400 E Woodcroft Parkway
Durham, NC

Prepared for:

Interlocking Concrete Pavement Institute

Updated August 7, 2015

Prepared by:

***Alessandra Smolek**, Ph.D. Student, North Carolina State University*

***William Hunt, III**, Ph.D., PE, D.WRE, Professor, Extension Specialist and University Faculty Scholar, North Carolina State University*

Table of Contents

List of Figures

List of Tables

EXECUTIVE SUMMARY

Permeable pavement is a commonly implemented stormwater control measure (SCM) for volume reduction and water quality mitigation in North Carolina. Multiple studies have shown permeable pavement is an effective tool to improve stormwater runoff hydrology and water quality when sited over Hydrologic Soil Group (HSG) A and B soils (Scholz and Grabwoiecki, 2007). Its efficacy over nearly impermeable soils (where volume reduction through infiltration is necessarily reduced) is less assured. To investigate this, North Carolina State University monitored the hydrologic mitigation and pollutant removal performance of a permeable pavement constructed over a low-infiltration, clay soil in Durham, NC from March 2014 through April 2015. Four parking stalls (540 ft^2) were retrofitted with permeable interlocking concrete pavement (PICP) to treat 1635 ft^2 of contributing impervious area (3:1 run-on ratio). Design of the permeable pavement followed typical design standards outlined in the North Carolina Department of Environment and Natural Resources (NCDENR) Best Management Practices Manual (NCDENR, 2012). In late September 2014, it was observed that a substantial portion of runoff was bypassing treatment along the curb adjacent to the permeable pavement. Subsequent monitoring of bypass volume determined 90% of the watershed was bypassing the system (Figure 4), reducing the treated watershed to 163.5 ft^2 and the run-on ratio to 0.3:1. All subsequent analyses were interpreted based on the post-construction watershed of the system. The site incorporated a six-inch internal water storage (IWS) zone to increase infiltration to the subsoil via an elevated underdrain. Flow-proportional water quality samples were obtained for untreated runoff and treated effluent and analyzed for the following pollutants: ammoniacal nitrogen (NH_3/NH_4^+-N), nitrate/nitrite-nitrogen (NO_3^-/NO_2^--N), total Kjeldahl nitrogen (TKN), total phosphorus (TP), soluble reactive phosphorus (SRP), total suspended solids (TSS), copper (Cu), lead (Pb), and zinc (Zn).

Results through thirteen months of monitoring show moderate volume reduction via subgrade infiltration and evaporation (22%) (Table 4); this was slightly higher than expected given the limited infiltration capacity of the subsoil and is attributed to the inclusion of the IWS zone. Inter-event drawdown of the IWS zone created storage to capture over 70% of the runoff volume from storm events less than 0.30 inches (Table 5), and peak flows were significantly reduced by a median of 84% (Table 6). The site exhibited exceptional pollutant removal efficiency, with influent and effluent pollutant concentrations significantly reduced for TSS (99%), TN (68%), and TP (96%) (Table 8). The median effluent concentrations of TN (0.52 mg/L) and TP (0.02 mg/L) were below

“excellent” ambient water quality thresholds for the Piedmont (McNett et al., 2010); the median TSS effluent concentrion was also very low (6.99 mg/L) and approaching irreducible concentrations. Additional sampling of the various nitrogen forms 12, 36, 60, and 84 hours post-rainfall was conducted to better understand mechanisms of nitrogen removal in permeable pavement; results from one storm event indicated denitrification is likely occurring in the internal water storage of the pavement. Significant event mean concentration reductions for the metals Cu (79%), Pb (92%) and Zn (88%) were also observed. Cumulative loading reduction for the watershed was excellent with loading removal efficiencies of 98%, 73% and 95% for TSS, TN, and TP, respectively. These results show permeable pavements built over low-infiltration, clay soils provide considerable improvement of water quality and moderate hydrologic mitigation.

Monitored data were also used to calibrate DRAINMOD, a widely-accepted agricultural drainage model, to predict the cumulative and event-by-event hydrologic performance of the study site. DRAINMOD accurately predicted runoff volumes from the impervious drainage area; NSEs exceeded 0.98 for the prediction of inflow during calibration and validation of the site. Good agreement between predicted and measured drainage was also observed, with NSEs of 0.72 and 0.92 during the calibration and validation periods, respectively. Modeled and measured agreement of infiltration and evaporation volumes was more varied; this is partially due to the low subgrade infiltration rates and therefore very small magnitude of infiltration volumes that occurred. Measured infiltration/evaporation volumes were so small in magnitude that any predicted deviation from the measured value resulted in a considerable percent error. Despite the storm-by-storm variability, the cumulative volume of infiltration/evaporation was predicted to within 8% of the measured volume over the course of the monitoring period. Similarly, cumulative predicted drainage volume was within 6% of what was measured during the monitoring period. These results indicate DRAINMOD can be applied to predict the water balance of permeable pavements built over low-infiltration, clay soils on a long-term, continuous basis.

PROJECT OVERVIEW

Permeable pavement is a low-impact stormwater control measure (SCM) which functions by reducing stormwater runoff volumes through storage in its aggregate layers and infiltration to the native soils. Research quantifying the hydrologic and water quality performance of permeable pavement applications constructed over nearly impermeable soils is limited. While permeable pavements consistently show surface runoff reductions greater than 99%, mostly permeable pavements built over sandier, more infiltrative Hydrologic Soil Group A and B soils have been studied extensively for runoff volume reduction through infiltration into the native soil (Collins et al., 2008; Wardynski et al., 2012). There is also little information on the water treatment capabilities of permeable pavements built to infiltrate into nearly impermeable soils, specifically with the inclusion of a saturated internal water storage (IWS) zone. Additionally, the hydrologic performance of a permeable pavement can vary based on design factors including drainage configuration (presence/lack of an underdrain, or inclusion of IWS), infiltration rate, impervious contributing run-on area, aggregate depth and underlying soil type. Since field-testing of every design configuration is not monetarily feasible, a long-term hydrologic model is needed to better understand the influence of these design variations on the hydrologic performance of permeable pavements. DRAINMOD is a widely accepted agricultural drainage model designed for low-gradient, tile drained fields (Skaggs, 1980). Past research has shown DRAINMOD can be calibrated to accurately predict the hydrology of bioretention areas with and without IWS zones (Brown et al., 2013). Given that both bioretention areas and permeable pavements employ infiltration and drainage as primary hydrologic mechanisms, it was hypothesized the model could also be calibrated to predict the hydrologic response from permeable pavement.

To investigate this, North Carolina State University ("NCSU") monitored a stormwater retrofit at Piney Woods Park in Durham, North Carolina to quantify hydrologic and water quality performance of permeable pavement built over low-infiltration, clay soils. Hydrologic data was also used to calibrate DRAINMOD to predict the hydrologic performance of the practice. These data will be combined with modeling results from four other sites in North Carolina and Ohio to create a comprehensive performance-based design tool for engineers, regulators, and industry.

SITE DESCRIPTION

The study site is located at Piney Wood Park on 400 E Woodcroft Parkway in Durham, North Carolina. Durham is a city in the Piedmont of North Carolina that receives 43.3 inches of rainfall per year (NOAA Station 152101, Raleigh-Durham International Airport). The site is located in the Cape Fear basin (9700 mi^2), Haw subbasin (1708 mi^2) and Crooked Creek watershed. The site is characterized by a triassic underlying soil (white store-urban land complex) with an average infiltration rate ranging from 0.00 to 0.06 in/hr.

Four parking stalls (540 ft^2) were retrofitted with permeable interlocking concrete pavement (PICP) to treat 1635 ft^2 of contributing impervious area (3:1 run-on ratio) (Fig. 1). Design followed typical hydrologic and structural standards for permeable pavement in North Carolina (NCDENR, 2012). The PICP profile consists of 15 inches of washed ASTM No. 2 aggregate subbase, 4 inches of washed ASTM No. 57 aggregate overlying the subbase, 2 inches of ASTM No. 87 aggregate, and 3.125 inch-thick concrete pavers with No. 87 stone filling their joints. To increase infiltration to the subsoil, the site incorporated a 6-inch internal water storage (IWS) zone via an elevated underdrain. The site was constructed in March 2014 and monitored continuously through April 2015. Sampling locations at a catch basin in the watershed and at the underdrain characterized hydrology and water quality of the influent and effluent runoff.

Figure 1. From left to right: (a) Aerial view of Piney Wood park: 540 ft^2 of PICP, 1635 ft^2 of contributing watershed area; (b) Piney Wood PICP retrofit.

Initially, a larger PICP footprint was retrofitted on the campus of North Carolina Central University, but the site was compromised for monitoring due to a crack in an old sewer pipe underlying the nearby pavement. This was the more hydraulically efficient pathway for the treated runoff to leave the system and subsequently, outflow was never observed from the underdrain. After discovering this within the first 1-2 months of monitoring, the new installation at Piney Wood was designed and constructed. To stay within budgetary constraints, the originally proposed 3000 ft^2 footprint of PICP was reduced to 540 ft^2.

DATA COLLECTION

Hydrology and Water Quality

Automated, flow-proportional ISCO 6712 water quality samplers (Teledyne Isco, Lincoln, Nebraska) were installed to determine water quality at a control site located on an adjacent parking lot and from the effluent leaving the underdrain (Fig. 2). To obtain flow-weighted composite samples from the control site, runoff from the adjacent parking lot (watershed size: 14,950 ft^2) was collected at an existing catch basin and measured using a sharp-crested 60° V-notch weir (Fig. 2). The entire throat of the catch basin was lined in an impermeable 45-mil ethylene propylene diene monomer (EPDM) rubber pond liner to ensure all runoff entered the stilling-area of the weir. A pressure transducer was fixed to the bottom of the stilling area to measure head and subsequent flow over the weir. Effluent from the system was measured directly by a 30° V-notch weir at the underdrain of the permeable pavement (Fig. 2). Flow measurements at the control and effluent were relayed to an ISCO 6712 automated sampler for flow-proportional aliquot sampling. Composite samples were collected within 24 hours after a storm event and submitted to the NCSU Center for Applied Aquatic Ecology for analysis of the event mean concentration (EMC) of the following parameters: total ammoniacal nitrogen (NH_3/NH_4^+-N), nitrate/nitrite-nitrogen (NO_3^-/NO_2^--N), total Kjeldahl nitrogen (TKN), total phosphorus (TP), soluble reactive phosphorus (SRP), total suspended solids (TSS), copper (Cu), lead (Pb), and zinc (Zn).

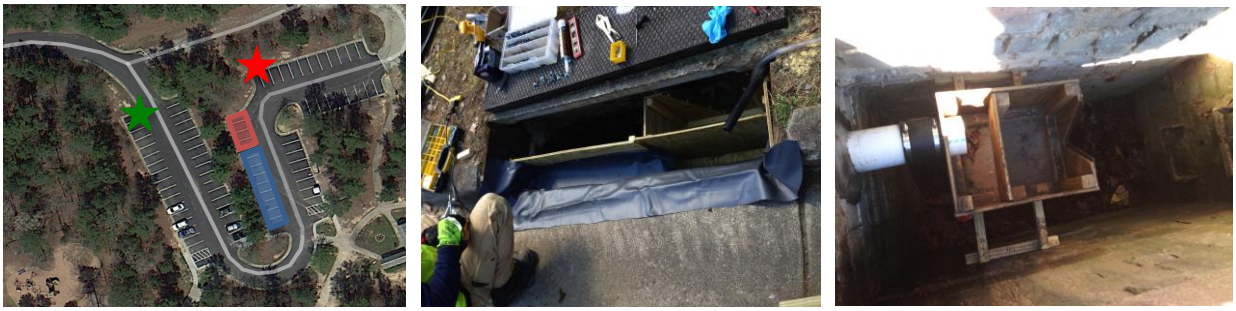

Figure 2. From left to right: (a) Aerial view of Piney Woods park: control sampling location (green star) and effluent sampling location (red star); (b) Control monitoring design; (c) Effluent monitoring design.

In September 2014, a portion of runoff from the contributing impervious area was observed bypassing the system along the curb of the permeable pavement. This was not a function of the surface being clogged, but rather a function of the contributing runoff flow path. The bypass formed a concentrated flow path at the catch basin downstream, where the effluent sampling location was installed. To assess what proportion of runoff from the contributing area was bypassing treatment, a third weir was installed at this location on October 1, 2014. An EPDM pond liner was used to ensure all runoff bypassing treatment entered the stilling area for measurement (Fig. 3). A HOBO U20 water level logger (Onset Computer Corporation, Bourne, MA) measured head over the 60° V-notch weir. Water level loggers also measured internal water level in the permeable pavement at two locations in the PICP. The loggers were housed in 1.25 in. wells that penetrated the aggregate base of the permeable pavement and into the subsoil. Atmospheric pressure was measured on site for accurate water level conversion. Rainfall at the site was measured using a tipping bucket rain gauge (0.01 inch/tip) and confirmed with a manual rain gauge.

Figure 3. Bypass monitoring design.

DRAINMOD Modeling

The four general fates of stormwater runoff routed through a permeable pavement include drainage outflow, infiltration to the surrounding subsoil, ET and surface runoff. To calibrate DRAINMOD to predict the percentage of stormwater runoff attaining each of these fates, weather, soil and drainage input parameters were measured onsite in addition to rainfall, drainage outflow and internal water level.

Weather inputs required to simulate DRAINMOD include hourly rainfall, minimum and maximum daily temperatures and the geographical location of the site (latitude and longitude). Minimum and maximum daily temperatures were obtained from the Raleigh-Durham Airport weather station (NC CRONOS). Latitude and longitude coordinates were obtained from the mapping program ArcGIS.

The soil preparation program embedded into DRAINMOD was used to develop Green-Ampt infiltration coefficients, water table depth-volume drained relationships and water table depth-upward flux relationships for the Piney Wood site. This program requires a user-specified soil-water characteristic curve, which explains how well a media holds water under increasing suction. One challenge in using DRAINMOD to predict permeable pavement hydrology is defining a soil-water characteristic representative of its highly porous stone media, which has a greater drainable porosity than the typical soil simulated by the model. Brown (2011) developed a reasonable estimation for a stone media by modifying a soil-water characteristic curve for a very sandy soil. This soil-water characteristic curve was used as the basis for calibration of the site.

The infiltration rate of the underlying soil is another essential parameter required to calibrate DRAINMOD. To determine the drawdown rate within the IWS, water level within the aggregate subbase of the permeable pavement application was measured using a HOBO U20 pressure transducer housed within a 1” diameter water table well. The change in stage during each dry period was multiplied by the effective porosity of the aggregate (0.35) and divided by drawdown time to characterize the overall rate of vertical infiltration, lateral infiltration, and evaporation occurring in the system. The average drawdown rate was used as the initial input for the deep seepage parameter in DRAINMOD.

Other soil-dependent and drainage parameters required to simulate DRAINMOD are listed in Table 1. The model is primarily calibrated by adjusting the soil characteristics starred in Table 1 based on measured data, including drainage outflow and internal water table depth.

As previously stated, drainage from the site was routed into a weir flow-measuring device equipped with a pressure transducer. Drainage volume was calculated using the measured pressure head and associated weir equation. Additionally, internal water level within the aggregate base of the permeable pavement was measured by piezometers at two locations in the PICP. The data obtained from these monitoring devices were used to compare modeled and field-measured results.

Table 1. Summary of equivalent permeable pavement design specifications for DRAINMOD inputs

DRAINMOD input	Permeable pavement design specifications
Depth from soil surface to drain	Depth from pavement surface to underdrain
Spacing between drains	Spacing between underdrains
Effective radius of drains	Underdrain size
Field ratio of contributing land area	Drainage area : permeable pavement area ratio
Vertical/deep seepage parameters*	Infiltration rate of the subsoil
Green-Ampt Parameters	Permeable pavement surface infiltration rate
Actual distance from surface to impermeable layer	Depth from pavement surface to bottom of aggregate
Drainage coefficient	Hydraulic drainage capacity of the cell
Inputs for soil-water characteristic curve*	Aggregate soil-water characteristic curve (Table 2) and aggregate depth
Lateral saturated hydraulic conductivity*	Lateral saturated hydraulic conductivity of aggregate

DATA ANALYSIS

Hydrology

Bypass monitoring began on October 1, 2014 and was used to determine the percentage of runoff bypassing the system, and subsequently, the area of the post-construction watershed treated by the permeable pavement. The NRCS Curve Number (CN) method was used to estimate the runoff generated from the designed impervious contributing area of 1635 ft^3 (NRCS, 1986):

$$Q = \frac{(P - 0.20 * S)^2}{P + 0.80 * S} * A_{Contrib} * C \quad (1)$$

where Q = runoff volume (ft^3), P = storm event precipitation depth (in), S = potential maximum retention (in) = $\frac{1000}{CN} - 10$, CN = Curve Number (98 for impervious cover), $A_{Contrib}$ = contributing watershed area (ft^2), C = conversion factor $\left(\frac{1\ ft}{12\ in}\right)$

Antecedent moisture corrections were applied to the CN for wet (antecedent dry period < 2 days) and dry (antecedent dry period > 5 days) conditions; wet conditions received a CN of 99, dry conditions utilized a CN of 94, and normal conditions used 98 for standard impervious cover (NRCS, 2004). From October 1, 2014 to April 15, 2014, the designed contributing area was estimated to generate 1700 ft^3 of runoff. Data from the bypass weir indicate during this same time, approximately 1530 ft^3 of contributing runoff bypassed the system. This indicates 90% of the contributing area runoff was bypassing the system, effectively reducing the contributing area from 1635 ft^2 to 163.5 ft^2, and the impervious run-on ratio from 3:1 to 0.3:1. The bypass was correlated moderately well to the storm precipitation depth (R^2=0.68, Figure 5). All subsequent analyses were computed considering the "true" contributing area of 163.5 ft^2.

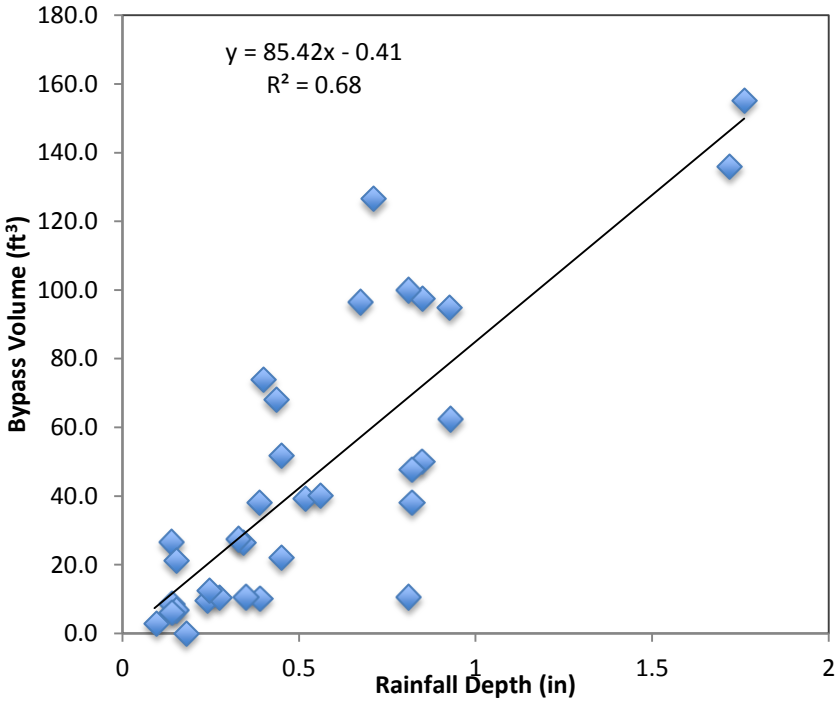

Figure 4. Bypass volume correlated to rainfall depth.

Discrete hydrologic storms were identified by a gap in precipitation exceeding six hours. To determine the runoff generated by the contributing watershed, the NRCS Curve Number method was used with antecedent moisture corrections as described in eq. 1 (NRCS, 2004). Direct rainfall volume on the PICP was added to the contributing area runoff to determine the total storm runoff volume (eq. 2).

$$V_T = Q + \frac{P}{12} * A_{PICP} \quad (2)$$

where V_T = total runoff volume (ft^3), Q = runoff generated from the 163.5 ft^2 of contributing area using eq. 1 with antecedent moisture corrections, P = precipitation (in.), and A_{PICP} = area of PICP (ft^2).

The average infiltration rate into the subsoil was determined by assessing the rate of drawdown of the water level within the two observation wells after drainage had ceased. It is noted, however, the infiltration rate may increase or decrease during a storm event due to changes in driving head and potential for lateral seepage and evaporation. Therefore, water losses due to infiltration and evaporation were calculated for each storm using a water balance (eq. 3).

$$V_T = V_D + V_{IE} + V_O \quad (3)$$

where V_T = total runoff volume from eq. 2 (ft^3), V_D = measured drainage (effluent) from the permeable pavement (ft^3), V_{IE}= volume of infiltration/evaporation (ft^3), and V_O = volume of overflow or surface runoff (ft^3). Since infiltration rates remained high throughout the course of the study, surface runoff was considered negligible.

Drainage from the PICP was measured directly at the underdrain. To calculate effluent runoff volumes from the raw weir level data, flow conversion was performed in FlowLink 5.1 (Teledyne-Isco, Lincoln, Nebraska).

Inter-event infiltration and evaporation was calculated by assessing the drawdown of the water level within the permeable pavement in between storm events. Drawdown was converted to a volume by multiplying the change in stage with the permeable pavement area and a porosity of 0.35. To account for intra-event infiltration, the total volume of inter-event infiltration was scaled up by the ratio of the

total monitoring period duration to the total inter-event period duration. Volume reduction through the system was assessed by comparing the calculated inflow volume to the PICP effluent volume.

Peak inflow runoff rates were also calculated using the Rational Method (Mulvany, 1851), a commonly used engineering method relating rainfall intensity to flow rate:

$$Q_p = C * i * A \tag{4}$$

where Q_p is the peak flow rate (ft^3/s), C is the rational coefficient, i is the peak 5-minute rainfall intensity measured during the storm (in/hr), and A is the watershed area (acres). The rational coefficient is customarily taken to be 0.95 for impervious areas (Chin 2006). Peak runoff reduction through the system was determined by comparing the peak inflow rates to the peak measured rates at the effluent.

Water Quality

Pollutant removal efficiencies for ammoniacal nitrogen (NH_3/NH_4^+-N), nitrate/nitrite-nitrogen (NO_3^-/NO_2^--N), total Kjeldahl nitrogen (TKN), total nitrogen (TN) total phosphorus (TP), soluble reactive phosphorus (SRP), and total suspended solids (TSS) were calculated on a storm event basis (eq. 5). TN was calculated by adding event mean concentrations (EMCs) of TKN and NO_3^-/NO_2^--N.

$$Removal\ Efficiency\ (\%) = \left(\frac{EMC_{ctrl,med} - EMC_{out,med}}{EMC_{ctrl,med}}\right) \times 100 \tag{5}$$

where $EMC_{crtl,med}$ = median control event mean concentration (mg/L) and $EMC_{out,med}$ = median outlet event mean concentration (mg/L) .

The control and effluent water quality data were log-transformed and checked for normality using the Shapiro-Wilk test and visual confirmation of residual plots. When data were normal, paired t-tests were performed to determine significant differences in control and effluent pollutant concentrations. Otherwise, the non-parametric Wilcoxon-Ranked signed-rank test was used to detect whether influent concentrations were significantly greater than control concentrations.

Cumulative load reduction through the PICP was also assessed by pairing event mean concentrations for TN, TP and TSS with measured flow data (eq. 6). Each EMC was paired with the stormwater volume pertinent to that sampling site for each storm. The load efficiency ratio was calculated by

summing the cumulative load in, the cumulative load out, and determining the percent reduction of those values:

$$Sum\ of\ Loads = 100 \times \left(1 - \frac{sum\ of\ outlet\ loads}{sum\ of\ inlet\ loads}\right) = 100 \times \left(1 - \frac{\sum_{i=1}^{n} EMC_{out,i} * V_{out,i}}{\sum_{i=1}^{n} EMC_{crtl,i} * V_{in,i}}\right) \quad (6)$$

where $EMC_{ctrl,i}$ = control EMC for event *i* (mg/L) and $EMC_{out,i}$ = outlet EMC for event *i* (mg/L), $V_{in,i}$ = total runoff volume for event *i*, $V_{out,i}$ = effluent volume for event *i*,. In this equation, the sum of outlet loads includes the underdrain outflow load only and did not consider any load associated with the bypassing volume from the original designed contributing area. Annual loading was determined on a lb/ac/yr basis by scaling up the cumulative effluent load using eq. 7. This loading was normalized by the total treated drainage area (163.5 ft^2 of contributing area and 540 ft^2 of PICP).

$$Annual\ Loading\ Export = \frac{\sum_{i=1}^{n} EMC_{out,i} * V_{out,i} * \frac{\sum V_{out,overall}}{\sum V_{out,WQ}}}{DA} * C \quad (7)$$

where $\sum V_{out,WQ}$ = sum of effluent volume sampled for water quality for one full year (ft^3), $\sum V_{out,overall}$ = total effluent volume measured for one full year (ft^3), DA = treated drainage area, and C = conversion factor to convert to lb/ac/yr.

DRAINMOD Modeling

After data was collected for one full year (March 2014 to February 2015), the model was primarily calibrated for each site by adjusting soil dependent variables based on monitored data. To ensure representation of the entire year of data (and to account for seasonal variability), storm events occurring during even months were used for model calibration. Calibration of the contributing area runoff was conducted first. Once modeled runoff was in acceptable agreement with the estimated runoff, the model was calibrated for the various forms of outflow (drainage, infiltration/evaporation and overflow). Nash-Sutcliffe Efficiencies (NSEs) for inflow, drainage, and infiltration/evaporation were calculated to measure model fit (eq. 8; Nash and Sutcliffe, 1970). An NSE of 1.0 represents perfect agreement between measured and modeled data; a model with an NSE of 0.0 or lower is no more accurate than predicting the mean value.

$$NSE = 1 - \frac{\sum_{i=1}^{N}\left(Q_{i,measured} - Q_{i,modeled}\right)^2}{\sum_{i=1}^{N}\left(Q_{i,measured} - Q_{average}\right)^2} \quad (8)$$

where $Q_{i,measured}$ = measured volume for event i, $Q_{i,modeled}$ = modeled volume for event i, and $Q_{average}$ = average measured volume for N events.

Upon calibration of the model, the model was validated by assessing model performance against measured data from odd months. Given the NSE can be sensitive to sample size, outlier values and bias, (McCuen et al., 2006; Jain and Sudheer, 2008), additional calculations of the coefficients of determination (R^2) and percent error of measured and predicted volumes were used to assess the goodness-of-fit for runoff and outflow variables holistically.

RESULTS

Hydrology

The average annual rainfall for Durham, NC is 43.3 inches (NOAA Station 152101). Through the first twelve months of monitoring (3/15/14 to 3/15/15), a total of 50.9 inches fell at the site; this is in the 89th percentile of annual rainfall recorded over the past 70 years. A summary of rainfall data collected over the entire thirteen month monitoring period is given in Table 2.

Table 2. Analysis of 66 hydrologic storm events from 3/15/14 to 4/15/15.

	Depth (in)	Storm Intensity (in/hr)	Storm Duration (hrs)	Catchment Peak Flow (cfs)	Antecedent Dry Period (days)
Min.	0.10	0.01	0.13	0.0043	0.3
Median	0.52	0.10	4.53	0.0157	4.5
Max.	4.12	2.41	34.73	0.1272	15.8
Average	0.73	0.28	7.66	0.0252	4.6
St. Dev.	0.73	0.44	7.81	0.0264	3.8

Water quality was measured for 29 storms. These storms tended to be larger than the overall hydrologic distribution, since storms less than 0.3" rarely produced outflow (Table 3).

Table 3. Analysis of storms for which water quality was measured (n = 14)

	Depth (in)	Storm Intensity (in/hr)	Storm Duration (hrs)	Catchment Peak Flow (cfs)	Antecedent Dry Period (days)
Min.	0.33	0.02	0.17	0.0044	0.3
Median	0.81	0.14	6.53	0.0296	5.0
Max.	3.52	2.41	32.17	0.1246	15.8
Average	0.99	0.33	8.74	0.0355	4.8
St. Dev.	0.73	0.54	8.20	0.0301	3.8

A summary of the hydrologic fate of the runoff treated by the permeable pavement is given in Table 4. 77% of the influent runoff received treatment and exited the PICP via the underdrain. The large percentage of drainage outflow is anticipated given the low infiltration rate of the HSG D underlying soil (0.00-0.06 in/hr); even with the inclusion of an IWS zone, volume reduction via infiltration was expected to be lower for this site compared to applications sited over higher conductivity soils. Analysis of the average rate of drawdown in the subbase after drainage had ceased confirmed the infiltration rate was low at 0.01 in/hr. Intra-event infiltration during the monitoring period was estimated by multiplying the measured inter-event infiltration by the ratio of the entire monitoring period to the inter-event period. Using this method, volume reduction by infiltration was determined to be about 22% of the overall water balance, leaving less than 1% of the runoff volume unaccounted for. This unaccounted volume is attributed to equipment error. A full summary of each storm can be found in Appendix A.

Table 4. Fate of runoff at Piney Woods for 74 storms from 3/15/14 to 4/15/14.

	Inflow	Outflow	Infiltration	Other
Total Volume (ft^3)	2919.4	2253.9	656.1	9.4
Percent of Inflow (%)	NA	77.2%	22.5%	0.3%
Duration (hrs)	566.7	1158.1	NA	NA

The average volume of inflow and outflow categorized by storm size is shown in Table 5. As storm size increased, a larger proportion of outflow as compared to inflow was observed. This indicates storm-by-storm volume reduction was greater for smaller storms. Even though the subgrade infiltration rate is very low, the average rate of infiltration (appx. 0.01 in/hr) shows the internal water storage zone could drawdown up to 1 inch in four days. Given the average antecedent dry period during the study was 4.5 days, inter-event drawdown created storage space to capture a larger percentage of the runoff for small storms less than 0.3 inches. Duration of outflow was typically less than 24 hours, indicating runoff drained from the subbase more quickly than the minimum 48 hours designated by NCDENR (2012). This is likely due to the portion of runoff bypassing the system; while the PICP was designed for a 3:1 impervious run-on ratio, the post-construction flow path of the contributing drainage area indicates the pavement was only receiving a 0.3:1 impervious run-on ratio and was subsequently oversized.

Table 5. Fate of runoff as a factor of storm size for 74 storms from 3/15/14 to 4/15/15.

Rainfall (in)	Average Duration of Outflow (hr)	Total Inflow (ft^3)	Total Outflow (ft^3)	Volume Reduction (%)
0.0-0.3	13.2	180.4	50.8	71.9
0.3-0.5	12.6	322.2	190.4	40.9
0.5-1.0	18.9	1025.6	822.7	19.8
>1.0	19.4	1391.2	1190.1	14.5

To estimate influent peak flow, the Rational Method was used as described in eq. 4. Influent and effluent peak flows were significantly reduced by a median of 84% [$p < 0.0001$ using the Wilcoxon non-parametric test (Fig. 5, Table 6)], which is comparable to other permeable pavement studies (Fassman and Blackbourn, 2010; Roseen et al., 2012). The effluent time to peak was extended on average by 0.39 hours, or 23 minutes, as compared to the influent time to peak. This is lower than the 0.50 to 2 hours reported in other studies (Brattebo and Booth, 2003; Collins et al., 2008, Fassman and Blackbourn, 2010), and is likely attributed to the low infiltration rate of the underlying soil.

Table 6. Summary of peak flow results for all hydrologic events (*n =74* storms)

Metric	Influent Peak Flow (cfs)	Effluent Peak Flow (cfs)	Peak Flow Reduction (%)	Lag to Peak (hr)
Median	0.015	0.003	84%	0.07
Mean	0.024	0.011	71%	0.39
St. Dev.	0.026	0.020	31%	2.3

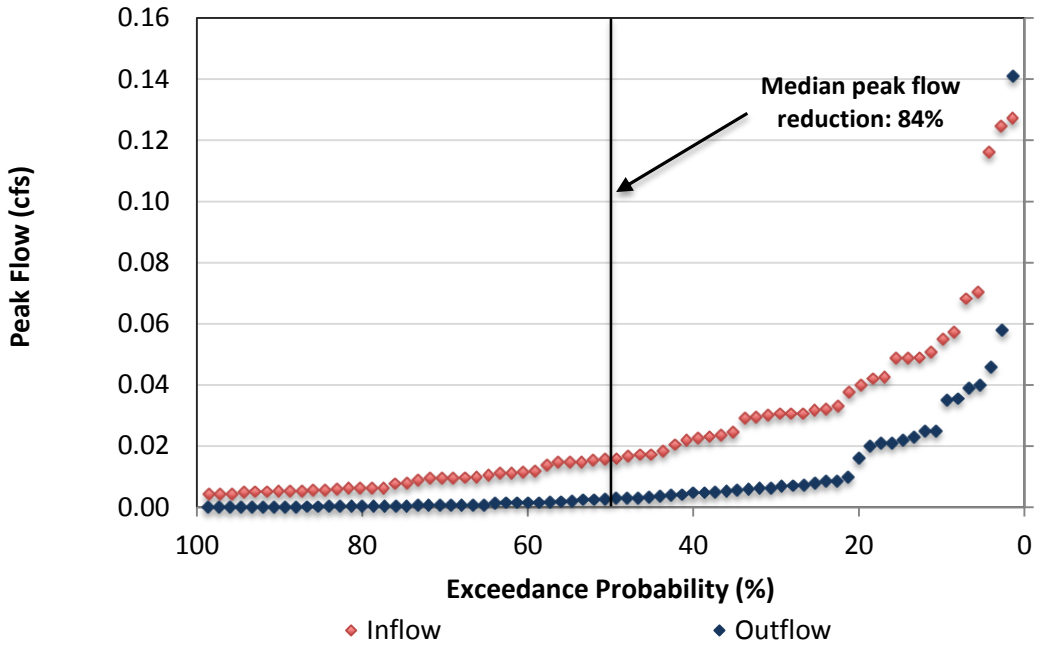

Figure 5. Influent and effluent peak flows for 74 storms from 3/15/14 to 4/15/15.

During the monitoring period, three storms had peak intensities exceeding the 1-yr, 5-min storm for Durham, NC (4.86 in/hr). Of these three storms, peak flow was mitigated 63% and 98% for two out of three storms; no peak flow mitigation was observed for the third storm. The third storm had a larger precipitation depth and an antecedent dry period less than 24 hours which likely contributed to the decreased peak flow mitigation. A summary of these three storms are given in Table 7.

Table 7. Summary of peak flow mitigation for three storm events with peak rainfall intensities exceeding the 1-yr, 5-min intensity for Durham, NC.

Date	Precipitation Depth (in)	5-min Peak Rainfall Intensity (in/hr)	Antecedent Dry Period (hr)	Peak Inflow (cfs)	Peak Outflow (cfs)	Peak Flow Reduction (%)
7/15/2014	3.52	7.64	19	0.116	0.141	-21
11/23/2014	0.82	8.20	132	0.125	0.046	63
3/1/2015	0.93	8.37	76	0.127	0.003	98

Water Quality

Twenty-nine paired storm events were sampled for ammoniacal nitrogen (NH_3/NH_4^+-N), nitrate/nitrite-nitrogen (NO_3^-/NO_2^--N), total Kjeldahl nitrogen (TKN), total phosphorus (TP), soluble reactive phosphorus (SRP), and total suspended solids (TSS). In general, data failed to fit normal or lognormal distributions, so the Wilcoxon signed-rank test was used. Table 7 summarizes all performance metrics for TSS, TN and TP for the PICP system. These primary pollutants of concern were all significantly reduced on an event mean concentration basis [$p \leq 0.0001$ using the Wilcoxon signed-rank test (Table 7)]. Removal efficiency was exceptionally high, resulting in an overall median removal efficiency of 98.8%, 68.4% and 96.5% for TSS, TN, and TP, respectively. These values generally exceed removal efficiencies for PICP reported in previous literature, though this is partially explained by high influent concentrations of TSS, TN and TP. These values also exceed the current permeable pavement pollutant removal regulatory credits designated for TSS (85%), TN (30%), and TP (35%) by the North Carolina Department of Environmental and Natural Resources (NCDENR, 2012).

Table 8. Summary of performance metrics for TSS, TN, and TP.

Evaluation Metric	Statistical Parameter	TSS	TN	TP
Event Mean Concentration (EMC)	n	28	29	28
	control mean [std. dev.] (mg/L)	703.2 [533.6]	2.04 [1.23]	0.50 [0.28]
	control median (mg/L)	568.3	1.65	0.44
	outlet mean [std. dev.] (mg/L)	14.7 [23.6]	0.65 [0.40]	0.03 [0.03]
	outlet median (mg/L)	7.0	0.52	0.02
	paired Wilcoxon p-values	**<0.0001**	**<0.0001**	**<0.0001**
EMC Percent Removal (all storms)	Removal Efficiency (based on median control and effluent concentrations)	98.8%	68.4%	96.5%
	mean	96.7%	61.9%	94.1%
	median	98.7%	68.1%	95.7%
	std. dev.	5.9%	26.9%	6.2%
	95% Conf. Int. (+/-)	2.1%	9.8%	2.2%
Individual Storm Load Reductions	Cum. Load Efficiency	98.3%	73.4%	95.3%
	mean	96.7%	71.8%	95.9%
	median	98.7%	78.0%	96.9%
	std. dev.	5.9%	26.0%	4.6%
	95% Conf. Int. (+/-)	2.1%	9.5%	1.7%

Cumulative probability plots for influent and effluent data of TN, TP and TSS are displayed in Fig. 6 and 7. The distributions of effluent concentrations for both TP and TSS were much lower and less varied than their respective control distributions; effluent concentrations of TN were varied but still visibly reduced. The dashed line in Fig. 5 represents the TN and TP pollutant concentrations corresponding to "excellent" ambient water quality for benthic macro-invertebrate health in the North Carolina Piedmont (McNett et al., 2010). These thresholds are 0.69 mg/L and 0.06 mg/L for TN and TP, respectively. The effluent TN concentration met the "excellent" target 65% of the time, while 85% of the measured TP effluent concentrations met the target. This indicates that despite influent concentrations being very high [and typically exceeding median levels reported in the National Stormwater Quality Database (Leisenring et al., 2014)], effluent concentrations for both TN and TP were consistently reduced to a level such that no threat existed to the health of receiving waters.

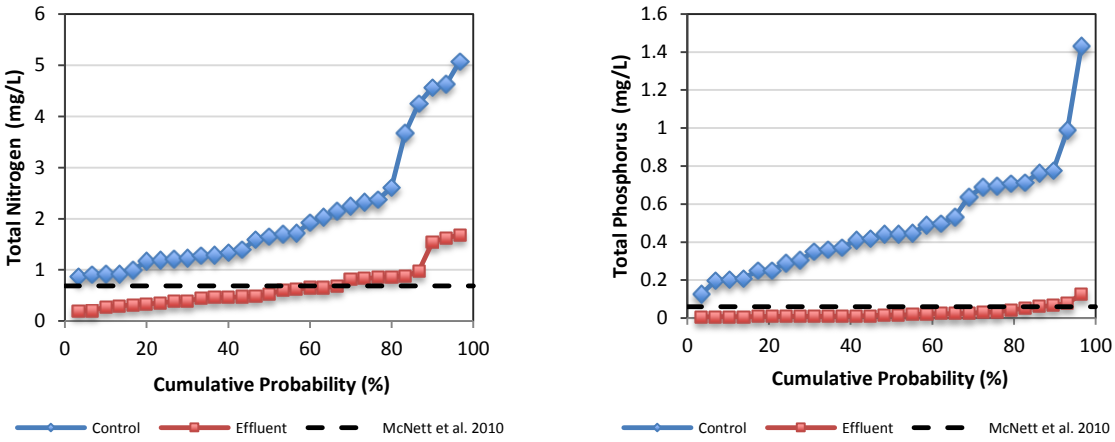

Figure 6. Left to right: Cumulative probability plots for control and effluent concentrations of (a) total nitrogen and (b) total phosphorus. Dashed line indicates "excellent" ambient water quality effluent concentration for the North Carolina Piedmont (McNett et al., 2010).

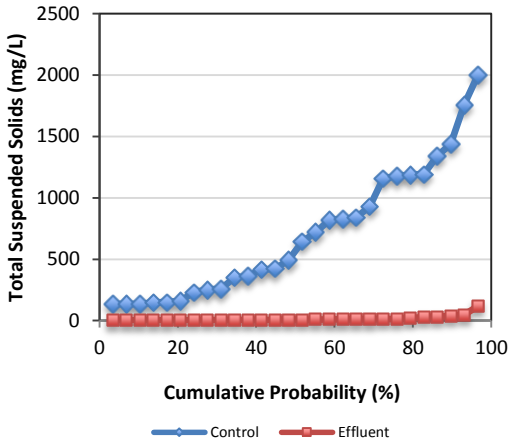

Figure 7. Cumulative probability plots for control and effluent concentrations of total suspended solids.

Other parameters measured include TKN, NO_3^-/NO_2^--N, NH_3/NH_4^+-N, and SRP. The concentrations of NH_3/NH_4^+-N were subtracted from TKN concentrations to determine the concentration of organic nitrogen (ON). A summary of performance metrics for these analytes is given in Table 9. The pollutant concentrations of ON, NH_3/NH_4^+-N and SRP were significantly reduced by 92%, 74% and 76%, respectively; the concentration of NO_3^-/NO_2^--N significantly increased. These results are typical of permeable pavements and are explained by the pollutant removal mechanisms employed by permeable pavement (primarily filtration and sedimentation). As shown in Fig. 8, a majority of the influent total nitrogen was in the form of particle-bound organic nitrogen; effluent nitrogen was primarily in the form of aqueous NO_3^-/NO_2^--N. While ON can readily be removed via filtration and sedimentation (and thus contribute to an overall reduction of TN when ON is the primary form), the increase in NO_3^-/NO_2^--N is attributed to nitrification of NH_3/NH_4^+-N (Bean et al., 2007, Collins et al., 2010). The removal of NO_3^-/NO_2^--N via denitrification requires anaerobic conditions, the presence of denitrifying bacteria, and a sufficient source of organic carbon (Birgand et al., 2007). During inter-event periods, anaerobic conditions were observed in the internal water storage zone (dissolved oxygen concentration ≈ 0 mg/L); however, as stormwater flowed through the PICP during storm events, dissolved oxygen concentrations rose to 8 mg/L. Because of this (as well as a potential lack of denitrifying bacteria and organic carbon), removal of NO_3^-/NO_2^--N via denitrification was not viable during storm events. SRP was removed at a very high rate (76%), despite the lack of an identifiable pollutant removal mechanism for the aqueous pollutant. A summary of all control and effluent pollutant concentrations is given in Appendix A.

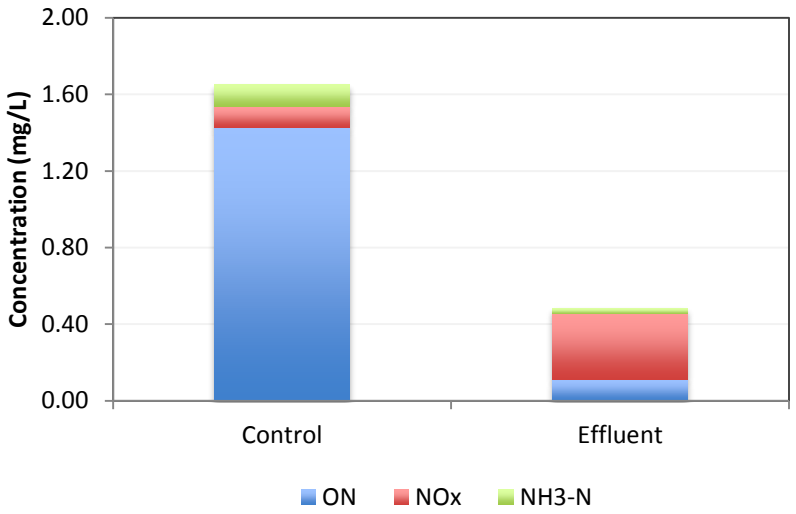

Figure 8. Average control and effluent concentrations for the various nitrogen forms.

Table 9. Summary of performance metrics for ON, NO_3^-/NO_2^--N, NH_3/NH_4^+-N, and SRP.

Evaluation Metric	Statistical Parameter	ON	NO_3^-/NO_2^--N	NH_3/NH_4^+-N	SRP
Event Mean Concentration (EMC)	n	29	29	29	29
	control mean [std. dev.] (mg/L)	1.79 [1.19]	0.13 [0.09]	0.13 [0.07]	0.0134 [0.0081]
	control median (mg/L)	1.43	0.11	0.12	0.0103
	outlet mean [std. dev.] (mg/L)	0.13 [0.07]	0.44 [0.26]	0.08 [0.18]	0.0033 [0.0023]
	outlet median (mg/L)	0.11	0.34	0.03	0.0025
	paired Wilcoxon p-values	**<0.0001**	**<0.0001**	**0.0006**	**<0.0001**
EMC Percent Removal (all storms)	Removal Efficiency (based on median control and effluent concentrations)	92.0%	-218.5%	74.4%	75.6%
	mean	90.5%	-518.0%	26.0%	72.6%
	median	91.8%	-230.6%	78.1%	71.0%
	std. dev.	6.5%	1145.1%	149.0%	17.1%
	95% Conf. Int. (+/-)	2.4%	416.8%	54.2%	6.2%
Individual Storm Load Reductions	Cum. Load Efficiency	93.2%	-148.6%	43.4%	79.9%
	mean	92.9%	-327.7%	37.1%	79.8%
	median	95.0%	-98.8%	84.5%	82.9%
	std. dev.	6.5%	727.3%	158.2%	11.8%
	95% Conf. Int. (+/-)	2.4%	264.7%	57.6%	4.3%

Considering a moderate percentage of the runoff volume of the stormwater received by the PICP infiltrated into the subgrade (over 22%), there is interest in the composition of the nitrogen infiltrating to the groundwater over time, particularly considering elevated levels of NO_3^-/NO_2^-N can cause methemoglobinemia and other health concerns (Anjana et al., 2006; Bryan and van Grinsen, 2013; Tricker and Preussmann 1991). Given that bioretention with IWS over less permeable soils exhibit denitrification potential (Passeport et al., 2009), and that low dissolved oxygen concentrations were observed inter-event in the IWS of the PICP (< 0.5 mg/L), it was hypothesized denitrification could be occurring in the subbase. While this was not explored extensively, the nitrogen composition of a flow-weighted effluent sample taken from a 0.38 inch storm event on 4/9/15 was compared to grab samples taken from the internal water storage zone at 12, 36, 60 and 84 hours after the end of the event. This is juxtaposed with the measured concentrations of dissolved oxygen in Fig. 9. It is apparent once dissolved oxygen decreased below 0.5 mg/L, the concentration of NO_3^-/NO_2^-N decreased as well, indicating presence of denitrifying bacteria and sufficient organic matter at the soil-water interface for denitrification to occur. The nitrate concentration within the IWS decreased from 0.68 mg/L to 0.04 mg/L between 12 and 36 hours after the storm and then further reduced to 0.02 mg/L at 60 hours and 84 hours. While definitive conclusions cannot be drawn from one storm event, these results suggest denitrification within the IWS of permeable pavements is a viable research area requiring further exploration.

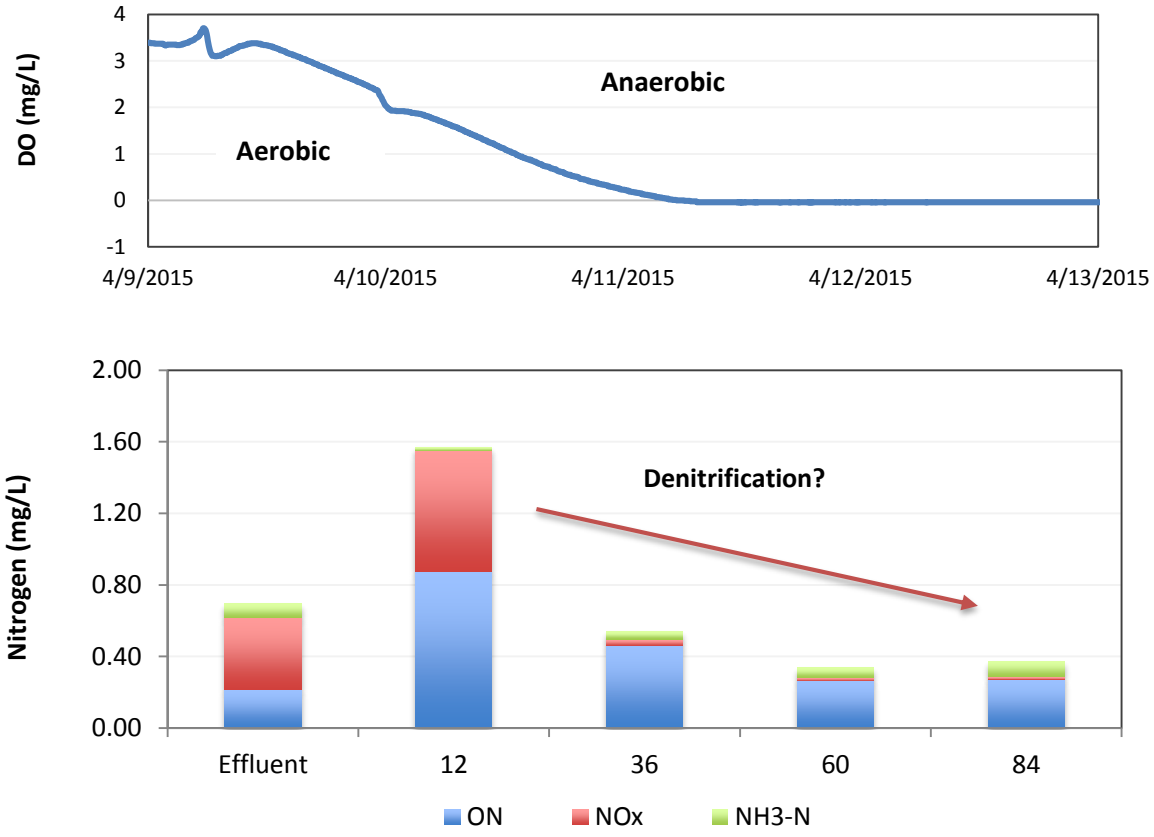

Figure 9. Nitrogen composition over time for grab samples obtained from IWS in a 0.38 inch storm occurring on 4/9/15.

Cumulative loading was assessed for TN, TP and TSS (Fig. 9). Loading efficiencies were exceptionally high, exceeding 95% for TSS and TP, and 70% for TN. From 3/15/14 to 3/15/15, 29 of 66 storms were sampled; the effluent volume sampled for water quality (1304 ft^3) represented approximately 60% of the total effluent volume during that time (2115 ft^3). This gives the author reasonable confidence in extrapolating cumulative loading to an annual export load. Export loadings were normalized by the treated drainage area and converted to lb/ac/year for each pollutant by extrapolating the cumulative loading by the quotient of the total effluent volume and the sampled water quality volume as described in eq. 7. Nearby Jordan Lake Rules target a maximum of 3.8 lb/ac/yr TN export and 1.4 lb/ac/yr TP export for new development (NCDENR 2012). While this target was met for TP, it was not met for TN, indicating high influent concentrations could not be mitigated to the standards required for nearby nutrient sensitive waters (Table 10).

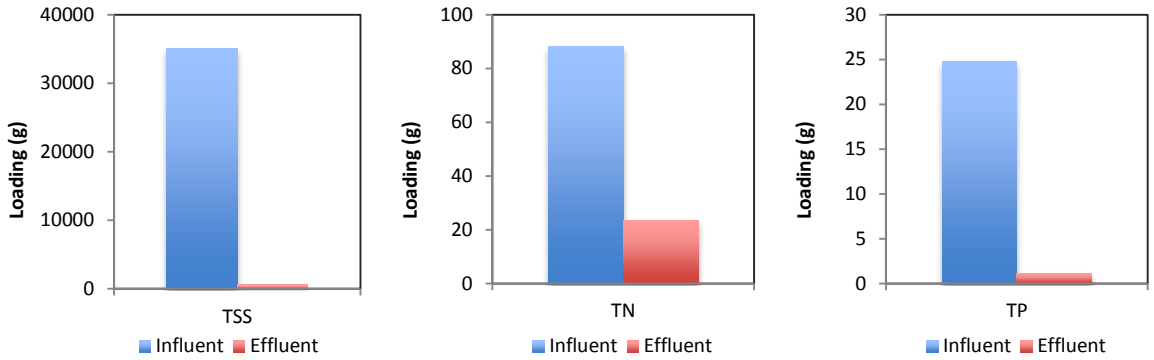

Figure 10. Influent and effluent cumulative loading for TSS, TN and TP.

Table 10. Annual loading for TSS, TN, and TP.

Pollutant	Annual Loading (lb/ac/yr)	
	Influent	**Effluent**
TSS	7549.6	123.4
TN	19.0	4.8
TP	5.3	0.2

Table 11 summarizes metals removal performance by the PICP, with all values reported as total metals (particulate-bound + dissolved). All metals were significantly reduced, and effluent concentrations were often reported below the minimum detection limit (MDL). 30% of the effluent Cu concentrations were below the MDL (2 µg/L), 100% of the effluent Pb concentrations were below the MDL (2 µg/L), and 95% of the effluent Zn concentrations were below the MDL (10 µg/L). This corresponded to median removal efficiencies of 79%, 92% and 88% for Cu, Pb, and Zn, respectively. Cumulative loading efficiency was also excellent, exceeding 85% for all three metals. Since dissolved metals were not analyzed, no conclusion can be made on the proportion of particulate-bound metals removed versus dissolved, but given the high removal rates it is expected a large proportion of the metals were in particulate-bound form.

Table 11. Summary of performance metrics for Cu, Pb, and Zn.

Evaluation Metric	Statistical Parameter	Cu	Pb	Zn
Event Mean Concentration (EMC)	n	19	19	19
	control mean [std. dev.] (µg/L)	15.3 [8.2]	13.5 [8.4]	51.3 [27.2]
	control median (µg/L)	11.0	12.0	41.0
	outlet mean [std. dev.] (µg/L)	3.2 [4.1]	< 2.0	5.3 [1.4]
	outlet median (µg/L)	2.3	< 2.0	5.0
	paired Wilcoxon p-values	**<0.0001**	**<0.0001**	**<0.0001**
EMC Percent Removal (all storms)	Removal Efficiency (based on median control and effluent concentrations)	79.1%	91.7%	87.8%
	mean	79.3%	87.7%	87.3%
	median	87.1%	93.3%	87.5%
	std. dev.	17.5%	10.8%	5.5%
	95% Conf. Int. (+/-)	7.9%	4.9%	2.5%
Individual Storm Load Reductions	Cum. Load Efficiency	87.1%	93.4%	90.4%
	mean	86.0%	91.2%	90.8%
	median	89.8%	93.8%	90.1%
	std. dev.	9.3%	7.5%	4.4%
	95% Conf. Int. (+/-)	4.2%	3.4%	2.0%

DRAINMOD Modeling

Given the site-by-site variability of hydrologic performance among practices, and the lack of funds to field-test every design configuration, it is intended that DRAINMOD is utilized to better understand the influence of these design variations on the annual hydrologic performance of permeable pavements (and most specifically, the volume mitigation provided by the practice). For these reasons, aggregated model predictions on an annual basis are far more relevant for the intended use of the model.

Results from the calibration and validation periods suggest DRAINMOD can be utilized to model the hydrologic response from permeable pavements with internal water storage zones and low-infiltration, clay soils (Table 12). The NSEs for inflow and drainage volume during the calibration period were 0.98 and 0.72, respectively. During the validation period, NSEs increased to 0.99 and 0.92 for inflow and drainage, respectively. Cumulative volumes for both inflow and drainage were within 6% during the calibration and validation periods. Given that the area of the subgrade (540 ft^2) was substantially larger than the area of the vertical side walls (81 ft^2) for this practice (as is the case for most permeable pavement practices with a shallow IWS zone), the measured drawdown rate of

0.01 in/hr (which represents combined vertical and lateral infiltration) was used to model infiltration. The cumulative volumes of infiltration/evaporation were predicted within 6% of what was measured during the calibration period and 30% of what was measured in the validation period. Despite relatively good agreement for cumulative infiltration/evaporation, this form of outflow was not predicted well on an event-by-event basis, with computed NSEs of -0.68 and -0.82 during calibration and validation, respectively. This is partially due to the very low subgrade infiltration rates and subsequently minimal amount of runoff volume lost via infiltration. Measured infiltration/evaporation volumes were so small in magnitude that any predicted deviation from the measured value resulted in a considerable percent error and thus more variability within the dataset. Additionally, the NSE can be sensitive to magnitude, sample size, outlier events, and bias (McCuen et al., 2006; Jain and Sudheer, 2008). Because of this, the NSE may not be the best measure of success for this hydrologic fate, especially considering cumulative model predictions are more relevant for the intended use of the model. Small differences in event-by-event prediction of infiltration/evaporation were evened out when aggregated over the course of the monitoring period.

This is confirmed by visual inspection of the cumulative drainage and infiltration/evaporation depths in Fig. 11, since the overall difference in both drainage volume and infiltration/evaporation during the monitoring period is minimal (and within 8%). Other sites across North Carolina and Ohio with varying drainage configurations and underlying soil types have exhibited similar calibration and validation results, with computed Nash Sutcliffe Efficiencies ranging from 0.36 to 0.99, and cumulative volumes for each hydrologic fate predicted within 10% of what was measured. These results suggest DRAINMOD is a viable model for prediction of annual permeable pavement hydrology.

Table 12. Summary of performance statistics for calibration and validation of the permeable pavement at Piney Wood Park.

Monitoring Period	**Method of Comparison**	**Fate of Runoff**: (cm per permeable pavement surface area over the monitoring period [percent of annual runoff])			
		Inflow	Drainage	Surface Runoff	Infiltration/Evap.
Calibration (April 2014, June 2014, August 2014, October 2014, December 2014, February 2015)	Measured/estimated volume	70	48 [70%]	0 [0%]	21 [30%]
	Modeled volume	71	51 [72%]	0 [0%]	20 [28%]
	Percent difference between measured and modeled water balance	-	2%	0%	-2%
	Percent difference between measured and modeled volumes	2%	6%	0%	-6%
	Nash-Sutcliffe Efficiency	0.98	0.72	-	-0.68
	Coefficient of Determination (r^2)	0.98	0.76	-	0.01
Validation (March 2014, May 2014, July 2014, September 2014, November 2014, January 2015)	Measured/estimated volume	78	65 [83%]	0 [0%]	13 [17%]
	Modeled volume	80	63 [79%]	0 [0%]	17 [21%]
	Percent difference between measured and modeled water balance	-	-4%	0%	4%
	Percent difference between measured and modeled volumes	3%	-3%	0%	29%
	Nash-Sutcliffe Efficiency	0.99	0.92	-	-0.82
	Coefficient of Determination (r^2)	1.00	0.92	-	0.04

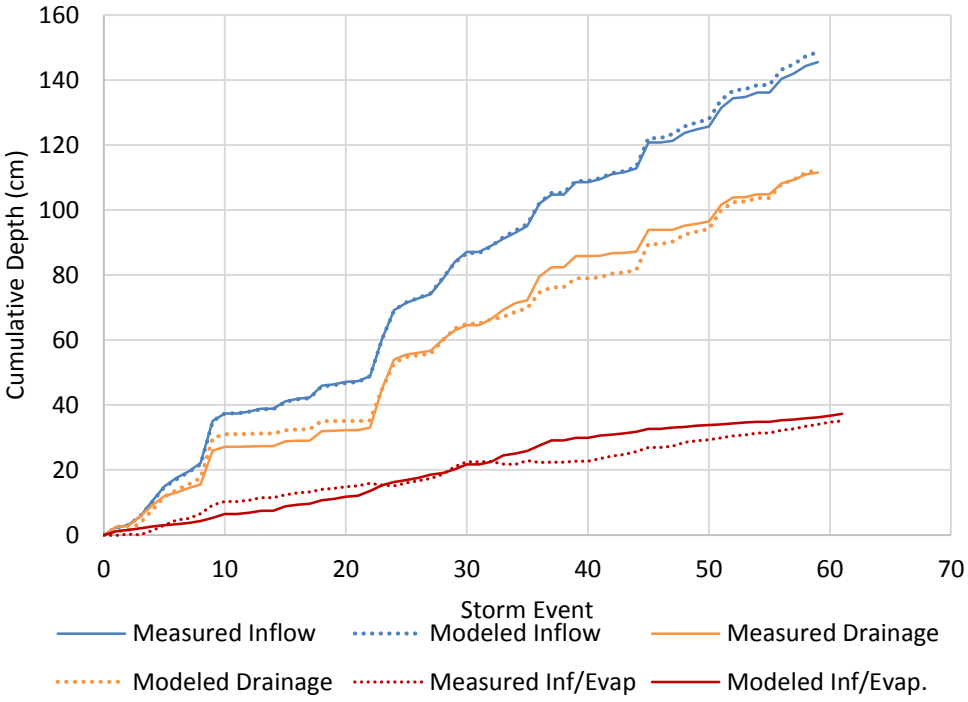

Figure 11. Measured and modeled cumulative inflow, drainage and infiltration/evaporation during from 3/15/14 to 3/15/15 for the Piney Woods permeable pavement site.

CONCLUSIONS AND RECOMMENDATIONS

Analyses show overall volume reduction via infiltration was moderate (appx. 22%) which was expected given the limitations of the underlying soil. Volume reduction was understandably lower than studies of permeable pavements built over infiltrative soils, but improved by the inclusion of an IWS zone. Other hydrologic benefits were observed within the system. Peak flows were effectively reduced by a median of 84% and storm events less than 0.3 inches exhibited greater capture of influent runoff than larger storms. Additionally, peak flows from two high-intensity events were adequately mitigated (63% and 98%).

Pollutant removal efficiencies were excellent and far exceeded the pollutant removal regulatory credits as designated in NCDENR, 2012, although this is partially attributed to high influent concentrations. Despite the high influent concentrations, effluent concentrations of TSS and TP were very low and did not vary much with influent concentrations; TN exhibited more variation but was still significantly reduced, meeting “excellent” ambient water quality thresholds 65% of the time (McNett et al. 2010). Sampling of the various nitrogen forms 12, 36, 60, and 84 hours post-rainfall

was conducted to better understand mechanisms of nitrogen removal; results from one storm event indicate denitrification may be occurring in the internal water storage of the pavement. While definitive conclusions cannot be drawn based on samples from one storm event, further exploration of denitrification within the IWS of permeable pavements is warranted. Concentrations of Cu, Pb, and Zn were significantly reduced by over 79%, 92% and 88%, respectively, and effluent concentrations were often below minimum detection limits. Cumulative loading reduction through the thirteen months of monitoring was also exceptional, exceeding 85% for TP, TSS, Cu, Pb, and Zn, and equivalent to 73% for TN. Despite these large reductions, the normalized annual export loading did not meet nearby TN standards for nutrient sensitive waters. The combination of these results show that permeable pavement built over low-infiltration, clay soils is a viable SCM for substantial improvement of water quality and moderate hydrologic mitigation.

DRAINMOD was used to simulate hydrologic performance from the permeable pavement over the course of the monitoring period. Results indicate DRAINMOD can be applied to predict the water balance of permeable pavements built over low-infiltration, clay soils on a long-term, continuous basis. Outputs included volumes of groundwater recharge (infiltration/evaporation), treated outflow (drainage), and untreated bypass (surface runoff). DRAINMOD accurately predicted runoff volumes from the highly impervious drainage area; NSEs exceeded 0.98 for the prediction of inflow during calibration and validation of the site. Good agreement between predicted and measured drainage was also observed, with NSEs of 0.72 and 0.92 during calibration and validation, respectively. Modeled and measured agreement of infiltration and evaporation volumes was more varied; this is partially due to the low subgrade infiltration rates and therefore very small magnitude of infiltration volumes that occurred. Despite this event-by-event variability, the total volume of infiltration and evaporation was predicted to within 8% of the measured volume over the course of the monitoring period. During the calibration and validation periods, cumulative predicted drainage volume was within 6% for both periods. Given the modeling success for other drainage configurations and underlying soil types in North Carolina and Ohio, DRAINMOD is expected to be an excellent option for long-term hydrologic modeling of permeable pavements.

REFERENCES

Anjana, S. U., Iqbal, M., & Abrol, Y. P. (2006). Are nitrate concentrations in leafy vegetables Within safe limits?. *Curr. Sci*, *90*, 58-64.

Bryan, N. S., & van Grinsven, H. (2013). The role of nitrate in human health. *Advances in Agronomy*, *119*, 153-82.

Birgand, F., Skaggs, R.W., Chescheir, G.M., Gilliam, J.W. (2007). Nitrogen removal in streams of agricultural catchments—A literature review. *Crit. Rev. Environ. Sci. Tech.*, 37(5), 381-487.

Brattebo, B. O., and Booth, D. B. (2003). Long-term stormwater quantity and quality performance of permeable pavement systems. *Water Res.*, 37(18), 4369-4376.

Bean, E. Z., Hunt, W. F. and Bidelspach, D. A. (2007). Evaluation of Four Permeable Pavement Sites in Eastern North Carolina for Runoff Reduction and Water Quality Impacts. *J. Irrig. Drain. Eng.*, 133(6), 583-592.

Brown, R.A. (2011). Evaluation of Bioretention Hydrology and Pollutant Removal in the Upper Coastal Plain of North Carolina with Development of a Bioretention Modeling Application in DRAINMOD. Ph.D. Dissertation, North Carolina State University, Raleigh, NC. <http:// repository.lib.ncsu.edu/ir/bitstream/1840.16/6783/1/etd.pdf>.

Brown, R.A., Skaggs, R.W. and Hunt, W.F. (2013). Calibration and Validation of DRAINMOD to Model Bioretention Hydrology. *J. Hydrol.*, 486, 430-442.

Booth, D. and Leavitt, J. (1999). Field Evaluation of Permeable Pavement Systems for Improved Stormwater Management. *J. Am. Plann. Assoc.*, 65(3), 314-325.

Chin, D.A. (2006). *Water resources engineering*. 2nd edition. Pearson Prentice Hall, Upper Saddle River, NJ.

Collins, K. A., Hunt, W. F. and Hathaway, J. M. (2008). Hydrologic Comparison of Four Types of Permeable Pavement and Standard Asphalt in Eastern North Carolina. *J. Hydrol. Eng.*, 13(12), 1146-1157.

Collins, K. A., Hunt, W.F., and Hathaway, J. M. (2010). Side-by-side comparison of nitrogen species removal for four types of permeable pavement and standard asphalt in eastern North Carolina. *J. Hydol. Eng.*, 15, 512-521.

Dreelin, E., Fowler, L. and Carroll, C. (2006). A Test of Porous Pavement Effectiveness on Clay Soils during Natural Storm Events. *Water Res.*, 40(4), 799-805.

Fassman, E. A. and Blackbourn, S. D. (2010). Urban Runoff Mitigation by a Permeable Pavement System Over Impermeable Soils. *J. Hydrol. Eng.*, 15(6), 475-485.

Jain, S.K., and Sudheer, K.P. (2008). "Fitting of hydrologic models: a close look at the Nash-Sutcliffe Index." *Journal of Hydrologic Engineering*, 13(10), 981-986

Leisenring, M., Clary, J., and Hobson, P. (2014). *International Stormwater Best Management Practices (BMP) Database Pollutant Category Statistical Summary Report.* International Stormwater BMP Database. (http://www.bmpdatabase.org/Docs/2014%20Water%20Quality%20Analysis%20Addendum/BMP%20Database%20Categorical_StatisticalSummaryReport_December2014.pdf).

McCuen, R.H., Knight, Z., Cutter, A.G. (2006). "Evaluation of the Nash-Sutcliffe Efficiency Index." *Journal of Hydrologic Engineering*, 11(6), 597-602.

McNett, J.K. W.F. Hunt, J.A. Osborne. 2010. Establishing Stormwater BMP Evaluation Metrics Based upon Ambient Water Quality Associated with Benthic Macro-invertebrate populations. *J. Environ. Eng.*, 136(5), 535-541.

Mulvany, T.J. (1851). "On the use of self-registering rain and flood gauges in making observations of the relation of rainfall and flood discharges in a given catchment." *Transactions of the Institution of Civil Engineers of Ireland*, 4, 18-33.

Nash, J.E., and Sutcliffe, J.V. (1970). "River flow forecasting through conceptual models part 1 – A discussion of principles." *Journal of Hydrology*, 10(3), 282-290.

National Oceanic and Atmospheric Administration (NOAA). (2015a). *National climatic data center, U.S. local climatological data*. Cleveland, OH airport. Available: http://www.ncdc.noaa.gov/

Natural Resource Conservation Service (NCRS). (2004). "Estimation of direct runoff from storm rainfall." *Hydrology: National engineering handbook*, Chapter 10, Part 360, Washington, DC.

Natural Resources Conservation Service (NRCS). (2004). *Urban hydrology for small watersheds*. Technical Release 55 (TR-55). 2nd edition. United States Department of Agriculture (USDA), Natural Resources Conservation Service, Conservation Engineering Division.

NCDENR. (2012). "Permeable Pavement." *Stormwater Best Management Practices Manual*. North Carolina Department of Environment and Natural Resources, Division of Water Quality.

Passeport, E., Hunt, W.F., Line, D.E., Smith, R.A., and Brown, R.A. (2009). "Field study of the ability of two grassed bioretention basins to reduce storm-water runoff pollution." *Journal of Irrigation and Drainage Engineering.* 135(4), 505-510.

Roseen, R. M., Ballestero, T. P., Houle, J. J., Briggs, J. F., Houle, K. M. (2012). Water Quality and Hydrologic Performance of a Porous Asphalt Pavement as a Storm-Water Treatment Strategy in a Cold Climate. *J. Environ. Eng.*, 138(1), 81-89.

Scholz, M., and Grabowiecki, P. (2007). "Review of Permeable Pavement Systems." *Build. Environ.*, 42(11), 3830-3836.

Tricker, A. R., & Preussmann, R. (1991). Carcinogenic N-nitrosamines in the diet: occurrence, formation, mechanisms and carcinogenic potential. *Mutation Research/Genetic Toxicology*, *259*(3), 277-289.

Skaggs, R. W. (1980). Methods for Design and Evaluation of Drainage-Water Management Systems for Soils with High Water Tables. DRAINMOD Reference Report. U.S. Department of Agriculture, Soil Conservation Service.

Wardynski, B. J., Winston, R. J. and Hunt, W. F. (2012). Internal water storage enhances exfiltration and thermal load reduction from permeable pavement in the North Carolina mountains. *J. Environ. Eng.*, 139(2), 18-195.

Appendix A

Table A1. Summary of runoff volume fate and peak flows for 74 hydrologic storms.

Date	Rainfall (in)	Storm Duration (hr)	Influent Volume (ft^3)	Effluent Volume (ft^3)	Inter-Event Infiltration Volume (ft^3)	Influent Peak Flow (cfs)	Effluent Peak Flow (cfs)
3/16/2014	0.73	34.7	41.2	44.2	14.2	0.0097	0.0015
3/23/2014	0.28	7.8	13.0	4.8	7.8	0.0426	<0.0001
3/28/2014	0.84	7.6	46.1	50.7	4.3	0.0221	0.0020
4/7/2014	1.46	3.9	83.9	61.3	10.4	0.0000	0.0080
4/15/2014	1.41	14.1	80.9	50.7	4.8	0.0000	0.0250
4/18/2014	0.82	24.9	46.4	18.9	5.8	0.0157	0.0009
4/25/2014	0.70	3.7	34.9	24.9	5.2	0.0703	0.0220
4/30/2014	0.82	9.9	45.1	18.9	9.3	0.0488	0.0063
5/15/2014	4.12	15.3	231.3	185.9	9.1	0.0550	0.0350
5/26/2014	0.38	0.5	17.9	7.9	1.9	0.0420	0.0042
5/27/2014	0.40	0.2	22.1	12.8	4.3	0.0377	0.0072
5/29/2014	0.19	0.2	9.9	2.1	5.6	0.0173	0.0006
6/9/2014	0.10	0.5	4.7	0.0	1.7	0.0116	<0.0001
6/9/2014	0.20	3.5	10.3	1.3	2.2	0.0063	0.0003
6/11/2014	0.74	3.5	41.7	25.4	2.6	0.0307	0.0086
6/12/2014	0.25	1.3	13.3	3.7	6.0	0.0185	0.0007
6/19/2014	0.14	2.0	6.3	0.5	1.3	0.0117	<0.0001
6/20/2014	1.15	6.5	65.7	52.4	5.2	0.0574	0.0356
6/25/2014	0.13	0.1	6.1	0.8	1.9	0.0149	<0.0001
6/27/2014	0.25	3.3	13.3	4.0	18.2	0.0099	0.0007
7/4/2014	0.11	0.2	5.0	0.1	15.1	0.0113	<0.0001
7/9/2014	0.57	4.1	27.9	14.2	1.9	0.0509	0.0070
7/15/2014	3.52	3.2	204.6	214.8	15.3	0.1161	0.1410
7/21/2014	2.78	7.0	153.4	156.7	3.7	0.0490	0.0580
7/24/2014	0.76	3.7	41.6	26.1	5.8	0.0321	0.0100
7/27/2014	0.44	0.3	23.5	10.6	5.4	0.0318	0.0037
7/31/2014	0.44	2.2	23.5	10.9	2.6	0.0307	0.0048
8/1/2014	1.43	11.2	82.1	60.1	10.2	0.0296	0.0160
8/9/2014	1.73	24.7	92.8	51.2	3.5	0.0205	0.0030
8/11/2014	0.52	9.5	28.9	11.3	0.4	0.0053	0.0009
8/12/2014	0.46	2.5	25.4	16.0	4.5	0.0153	0.0033
8/18/2014	0.68	1.1	33.8	33.6	6.7	0.0487	0.0200
8/23/2014	0.69	0.5	37.5	50.8	5.6	0.0401	0.0400
8/29/2014	0.68	0.5	33.8	36.0	7.3	0.0331	0.0210
9/8/2014	0.65	-[a]	36.5	15.8	7.3	0.0000	0.0007
9/23/2014	2.10	32.2	121.3	130.3	9.1	0.0301	0.0230

10/10/2014	0.85	4.2	43.2	43.5	4.1	0.0682	0.0250
10/11/2014	0.14	0.7	7.0	6.3	4.5	0.0168	0.0007
10/14/2014	0.40	1.8	21.1	16.8	1.7	0.0227	0.0050
10/15/2014	0.81	7.0	45.6	44.4	19.2	0.0173	0.0060
10/29/2014	0.34	5.7	16.0	2.3	7.3	0.0237	0.0003
11/1/2014	0.52	6.4	27.7	13.4	5.0	0.0062	0.0026
11/6/2014	0.24	7.8	11.0	1.6	14.3	0.0088	0.0003
11/17/2014	0.45	8.1	21.6	6.9	6.7	0.0148	0.0016
11/23/2014	0.82	0.5	41.5	41.4	0.6	0.1246	0.0460
11/25/2014	1.72	16.8	99.1	76.5	7.6	0.0106	0.0064
12/6/2014	0.18	9.5	8.1	0.1	4.1	0.0051	0.0000
12/8/2014	0.81	22.6	44.5	23.7	16.3	0.0044	0.0025
12/16/2014	0.39	1.9	18.5	9.8	14.6	0.0149	0.0017
12/22/2014	0.35	6.1	16.5	11.7	3.0	0.0053	0.0019
12/23/2014	1.76	20.1	101.5	90.6	3.9	0.0139	0.0071
12/29/2014	0.93	11.5	51.3	41.4	7.6	0.0054	0.0030
1/3/2015	0.14	2.7	6.7	1.3	1.3	0.0043	0.0003
1/4/2015	0.33	13.2	17.8	10.5	0.4	0.0246	0.0054
1/4/2015	0.15	4.5	7.8	4.4	10.8	0.0096	0.0008
1/12/2015	1.41	16.5	74.6	59.6	14.5	0.0079	0.0056
1/18/2015	0.56	4.2	27.4	19.4	4.1	0.0159	0.0040
1/23/2015	0.85	24.4	43.0	30.1	6.7	0.0055	0.0016
2/2/2015	0.44	7.7	20.9	10.1	19.5	0.0112	0.0030
2/9/2015	0.82	16.8	41.5	29.7	7.1	0.0061	0.0016
2/22/2015	0.27	1.7	12.7	5.2	6.5	0.0096	0.0003
2/26/2015	0.27	4.5	14.0	6.5	0.0	0.0096	0.0002
2/27/2015	0.32	2.3	17.2	14.3	0.0	0.0077	0.0016
3/1/2015	0.93	2.3	52.8	25.7	3.0	0.1272	0.0025
3/5/2015	0.71	9.9	40.1	53.1	3.0	0.0051	0.0048
3/13/2015	0.30	20.3	14.2	4.9	12.2	0.0051	0.0004
3/19/2015	0.70	14.7	34.9	28.9	15.1	0.0062	NA[a]
3/25/2015	0.15	6.2	6.9	1.4	0.0	0.0064	0.0004
3/27/2015	0.25	9.0	13.1	6.1	3.7	0.0043	0.0006
3/30/2015	0.14	1.6	6.7	0.6	21.5	0.0043	0.0001
4/7/2015	0.10	11.0	4.4	0.0	3.0	0.0055	0.0000
4/9/2015	0.39	1.3	21.2	18.0	1.1	0.0232	0.0086
4/9/2015	0.45	4.6	24.9	26.9	12.6	0.0292	0.0210
4/14/2015	0.67	4.1	36.6	57.0	1.6	0.0307	0.0390
SUM	**53.7**	**560.7**	**2919.4**	**2253.9**	**656.1[b]**		

[a]Lost data due to equipment malfunction
[b]Total also includes intra-event infiltration

Table A2. Summary of control and effluent pollutant concentrations of nitrogen species for 29 water quality storms.

Date	TKN (mg/L)		NOx (mg/L)		NH3-N (mg/L)		TN (mg/L)	
	Control	Effluent	Control	Effluent	Control	Effluent	Control	Effluent
3/28/2014	1.17278	1.18193	0.11082	0.36216	0.11143	0.85452	1.28360	1.54409
4/7/2014	1.22608	0.74614	0.16806	0.93432	0.17780	0.57432	1.39414	1.68046
4/15/2014	4.60624	0.32089	0.02031	1.30644	0.04401	0.07645	4.62655	1.62733
4/25/2014	5.0108	0.26017	0.06149	0.61196	0.16200	0.05349	5.07229	0.87213
4/30/2014	2.02462	0.22557	0.12365	0.64088	0.08109	0.03001	2.14827	0.86645
5/27/2014	3.34614	0.17798	0.32813	0.65392	0.22578	0.04644	3.67427	0.8319
6/11/2014	2.37186	0.13154	0.24096	0.71844	0.12306	0.00992	2.61282	0.84998
6/20/2014	1.6598	0.17844	0.26583	0.50472	0.13814	0.01331	1.92563	0.68316
7/9/2014	4.24704	0.21143	0.31658	0.6028	0.37082	0.04456	4.56362	0.81423
7/15/2014	2.05314	0.24752	0.19333	0.22919	0.18798	0.05096	2.24647	0.47671
7/21/2014	1.1492	0.12998	0.14286	0.25902	0.16484	0.02725	1.29206	0.389
7/24/2014	1.06618	0.09776	0.13039	0.2837	0.22024	0.01263	1.19657	0.38146
8/1/2014	0.88126	0.12525	0.04263	0.33968	0.12806	0.01505	0.92389	0.46493
8/9/2014	1.1407	0.11234	0.0962	0.53808	0.06749	0.01475	1.2369	0.65042
8/12/2014	2.21394	0.12094	0.11375	0.32762	0.21901	0.03163	2.32769	0.44856
8/18/2014	1.93154	0.17502	0.09486	0.34666	0.11503	0.02492	2.0264	0.52168
9/23/2014	0.82792	0.1354	0.04482	0.32236	0.03639	0.0215	0.87274	0.45776
10/10/2014	2.12242	0.11469	0.24855	0.49068	0.11724	0.01486	2.37097	0.60537
10/14/2014	0.96521	0.15116	0.02863	0.2044	0.07914	0.04327	0.99384	0.35556
11/1/2014	1.07804	0.27828	0.26545	0.69384	0.1259	0.08062	1.34349	0.97212
11/17/2014	1.56934	0.12139	0.13133	0.50372	0.05248	0.02093	1.70067	0.62511
11/23/2014	0.8903	0.08941	0.0195	0.1832	0.03333	0.03699	0.9098	0.27261
12/8/2014	1.57914	0.12025	0.07208	0.19594	0.15402	0.05309	1.65122	0.31619
12/16/2014	1.07033	0.05263	0.10201	0.15042	0.10471	0.01485	1.17234	0.20305
1/4/2015	4.2366	0.06592	0.0171	0.13364	0.05265	0.00892	4.2537	0.19956
1/12/2015	1.51734	0.05575	0.07192	0.23774	0.08925	0.01686	1.58926	0.29349
1/23/2015	1.10166	0.0606	0.10664	0.26996	0.1236	0.01371	1.2083	0.33056
2/2/2015	1.61862	0.32158	0.09917	0.33114	0.08403	0.04754	1.71779	0.65272
2/9/2015	0.84132	0.19345	0.08315	0.29494	0.04427	0.06646	0.92447	0.48839
Average	1.91447	0.21391	0.12897	0.43695	0.12530	0.07999	2.04344	0.65086
Median	1.56934	0.13540	0.10664	0.33968	0.11724	0.03001	1.65122	0.52168

Table A3. Summary of control and effluent pollutant concentrations of phosphorus, soluble reactive phosphorus, and total suspended solids for 29 water quality storms.

Date	TP (mg/L)		SRP (mg/L)		TSS (mg/L)	
	Control	Effluent	Control	Effluent	Control	Effluent
3/28/2014	0.20978	0.01134	0.00902	0.00189	136.51	2.92
4/7/2014	0.41938	0.02348	0.01444	0.00476	260.2	8.27
4/15/2014	0.68940	0.05110	0.00749	0.00205	719.44	19.8
4/25/2014	1.4306	0.06075	0.01339	0.00473	2000.25	47.85
4/30/2014	0.37062	0.04270	0.00624	0.00319	929.77	29.55
5/27/2014	0.71405	0.02425	0.01855	0.00517	1186.73	12.09
6/11/2014	0.6961	0.00925	0.00558	0.00199	818.25	5.02
6/20/2014	0.63916	0.00883	0.00622	0.00124	1158.37	3.14
7/9/2014	0.4416	0.00978	0.00746	0.00197	1175.15	6.92
7/15/2014	0.98788	0.07738	0.00832	0.00251	1758.08	30.08
7/21/2014	0.70928	0.03125	0.01753	0.00611	829.43	5.44
7/24/2014	0.77704	0.03125	0.01689	0.00207	643.86	9.23
8/1/2014	0.44768	0.0237	0.00832	0.00339	492.81	4.25
8/9/2014	0.36048	0.00871	0.00759	0.00234	349.59	7.06
8/12/2014	0.76464	0.00569	0.01497	0.01278	1192.22	3.18
8/18/2014	NA[a]	0.01304	0.00615	0.00299	1340.91	5.48
9/23/2014	0.3048	0.01117	0.0138	0.00186	363.57	2.15
10/10/2014	0.53224	0.02264	0.00849	0.00181	1438.24	4.94
10/14/2014	0.49084	0.00837	0.00849	0.00181	416.27	1.33
11/1/2014	0.2486	0.0166	0.01018	0.00341	136.59	9.76
11/17/2014	0.41108	0.01869	0.03285	0.00232	NA[b]	NA[b]
11/23/2014	0.29051	0.06751	0.03611	0.00749	231.47	38.45
12/8/2014	0.24972	0.01227	0.02417	0.00352	148.22	9.84
12/16/2014	0.34976	0.00785	0.0213	0.00337	252.36	9.32
1/4/2015	0.4974	0.01566	0.01159	0.00378	840.14	13.13
1/12/2015	0.20412	0.00741	0.02501	0.00218	149.92	1.85
1/23/2015	0.19664	0.00898	0.01481	0.00093	136.11	0.96
2/2/2015	0.44212	0.12658	0.0041	0.00257	422.89	119.21
2/9/2015	0.12577	0.00734	0.01028	0.00231	161.46	1.51
Average	0.50005	0.02633	0.01343	0.00333	703.17	14.74
Median	0.44186	0.01566	0.01028	0.00251	568.34	6.99

[a]Analysis from lab invalid due to violation of quality control for this sample
[b]Insufficent volume for TSS analysis for this storm event

Table A4. Summary of control and effluent pollutant concentrations of copper, lead, and zinc for 19 water quality storms.

Date	Cu (µg/L)		Pb (µg/L)		Zn (µg/L)	
	Control	Effluent	Control	Effluent	Control	Effluent
4/30/2014	21	3.7	20	<2.0	61	11
5/27/2014	28	2.3	25	<2.0	78	<10.0
6/11/2014	21	2.7	19	<2.0	65	<10.0
6/20/2014	14	2.3	15	<2.0	39	<10.0
7/15/2014	14	2.4	16	<2.0	48	<10.0
7/21/2014	10	<2.0	12	<2.0	35	<10.0
7/24/2014	11	<2.0	11	<2.0	41	<10.0
8/1/2014	10	<2.0	9.1	<2.0	28	<10.0
8/9/2014	9.3	<2.0	6.9	<2.0	25	<10.0
8/12/2014	36	19	33	<2.0	99	<10.0
8/18/2014	18	2.9	16	<2.0	49	<10.0
9/23/2014	7.8	<2.0	6.6	<2.0	34	<10.0
10/10/2014	24	2	25	<2.0	100	<10.0
10/14/2014	11	2.9	8.6	<2.0	40	<10.0
12/8/2014	7.5	2.5	3.3	<2.0	28	<10.0
1/4/2015	24	2.3	18	<2.0	110	<10.0
1/12/2015	8.5	<2.0	4.2	<2.0	27	<10.0
1/23/2015	6.1	2.1	2.2	<2.0	22	<10.0
2/2/2015	10	7.5	5.4	<2.0	45	<10.0
Average	15.3	3.2*	13.5	1.0*	51.3	5.3*
Median	11.0	2.3*	12.0	1.0*	41.0	5.0*

*When reported values were below the minimum detection limit, half the minimum detection limit was used for storm-by-storm comparisons and computation of the mean and median.

Appendix B

R code for normality and statistical significance:

```
> shapiro.test(PineyPoll$TSS.Ctrl)

        Shapiro-Wilk normality test

data:  PineyPoll$TSS.Ctrl
W = 0.8984, p-value = 0.01051

> shapiro.test(PineyPoll$TSS.Out)

        Shapiro-Wilk normality test

data:  PineyPoll$TSS.Out
W = 0.5569, p-value = 4.637e-08

> shapiro.test(PineyPoll$TN.Ctrl)

        Shapiro-Wilk normality test

data:  PineyPoll$TN.Ctrl
W = 0.808, p-value = 0.0001167

> shapiro.test(PineyPoll$TN.Out)

        Shapiro-Wilk normality test

data:  PineyPoll$TN.Out
W = 0.8409, p-value = 0.0004976

> shapiro.test(PineyPoll$TP.Ctrl)

        Shapiro-Wilk normality test

data:  PineyPoll$TP.Ctrl
W = 0.89, p-value = 0.006716

> shapiro.test(PineyPoll$TP.Out)

        Shapiro-Wilk normality test

data:  PineyPoll$TP.Out
W = 0.7166, p-value = 3.677e-06

> shapiro.test(PineyPoll$NOX.Cntrl)

        Shapiro-Wilk normality test

data:  PineyPoll$NOX.Cntrl
W = 0.9042, p-value = 0.01236

> shapiro.test(PineyPoll$NOX.Out)

        Shapiro-Wilk normality test

data:  PineyPoll$NOX.Out
W = 0.8661, p-value = 0.001663

> shapiro.test(PineyPoll$NH3.Ctrl)

        Shapiro-Wilk normality test
```

```
data:  PineyPoll$NH3.Ctrl
W = 0.8973, p-value = 0.00843

> shapiro.test(PineyPoll$NH3.Out)

        Shapiro-Wilk normality test

data:  PineyPoll$NH3.Out
W = 0.3834, p-value = 5.742e-10

> shapiro.test(PineyPoll$NOX.Cntrl)

        Shapiro-Wilk normality test

data:  PineyPoll$NOX.Cntrl
W = 0.9042, p-value = 0.01236

> shapiro.test(PineyPoll$NOX.Out)

        Shapiro-Wilk normality test

data:  PineyPoll$NOX.Out
W = 0.8661, p-value = 0.001663

> shapiro.test(PineyPoll$Ortho.Ctrl)

        Shapiro-Wilk normality test

data:  PineyPoll$Ortho.Ctrl
W = 0.8601, p-value = 0.001233

> shapiro.test(PineyPoll$Ortho.Out)

        Shapiro-Wilk normality test

data:  PineyPoll$Ortho.Out
W = 0.7218, p-value = 4.392e-06

> shapiro.test(ON.Ctrl)

        Shapiro-Wilk normality test

data:  ON.Ctrl
W = 0.7779, p-value = 3.434e-05

> shapiro.test(ON.Out)

        Shapiro-Wilk normality test

data:  ON.Out
W = 0.9366, p-value = 0.08181

> shapiro.test(PineyPoll$Cu.Ctrl)

        Shapiro-Wilk normality test

data:  PineyPoll$Cu.Ctrl
W = 0.8772, p-value = 0.01919

> shapiro.test(PineyPoll$Cu.Out)

        Shapiro-Wilk normality test

data:  PineyPoll$Cu.Out
```

```
W = 0.5083, p-value = 5.948e-07

> shapiro.test(PineyPoll$Pb.Ctrl)

        Shapiro-Wilk normality test

data:  PineyPoll$Pb.Ctrl
W = 0.9484, p-value = 0.3716

> shapiro.test(PineyPoll$Pb.Out)
Error in shapiro.test(PineyPoll$Pb.Out) : all 'x' values are identical
> shapiro.test(PineyPoll$Zn.Ctrl)

        Shapiro-Wilk normality test

data:  PineyPoll$Zn.Ctrl
W = 0.856, p-value = 0.008411

> shapiro.test(PineyPoll$Zn.Out)

        Shapiro-Wilk normality test

data:  PineyPoll$Zn.Out
W = 0.2439, p-value = 5.28e-09

> shapiro.test(log(PineyPoll$TSS.Ctrl))

        Shapiro-Wilk normality test

data:  log(PineyPoll$TSS.Ctrl)
W = 0.9216, p-value = 0.0379

> shapiro.test(log(PineyPoll$TSS.Out))

        Shapiro-Wilk normality test

data:  log(PineyPoll$TSS.Out)
W = 0.9788, p-value = 0.8209

> shapiro.test(log(PineyPoll$TN.Ctrl))

        Shapiro-Wilk normality test

data:  log(PineyPoll$TN.Ctrl)
W = 0.9244, p-value = 0.03943

> shapiro.test(log(PineyPoll$TN.Out))

        Shapiro-Wilk normality test

data:  log(PineyPoll$TN.Out)
W = 0.9723, p-value = 0.6234

> shapiro.test(log(PineyPoll$TP.Ctrl))

        Shapiro-Wilk normality test

data:  log(PineyPoll$TP.Ctrl)
W = 0.9869, p-value = 0.9721

> shapiro.test(log(PineyPoll$TP.Out))

        Shapiro-Wilk normality test
```

```
data:  log(PineyPoll$TP.Out)
W = 0.9282, p-value = 0.04939

> shapiro.test(log(PineyPoll$NOX.Cntrl))

        Shapiro-Wilk normality test

data:  log(PineyPoll$NOX.Cntrl)
W = 0.9393, p-value = 0.09598

> shapiro.test(log(PineyPoll$NOX.Out))

        Shapiro-Wilk normality test

data:  log(PineyPoll$NOX.Out)
W = 0.9805, p-value = 0.8518

> shapiro.test(log(PineyPoll$NH3.Ctrl))

        Shapiro-Wilk normality test

data:  log(PineyPoll$NH3.Ctrl)
W = 0.9716, p-value = 0.604

> shapiro.test(log(PineyPoll$NH3.Out))

        Shapiro-Wilk normality test

data:  log(PineyPoll$NH3.Out)
W = 0.8481, p-value = 0.000694

> shapiro.test(log(PineyPoll$NOX.Cntrl))

        Shapiro-Wilk normality test

data:  log(PineyPoll$NOX.Cntrl)
W = 0.9393, p-value = 0.09598

> shapiro.test(log(PineyPoll$NOX.Out))

        Shapiro-Wilk normality test

data:  log(PineyPoll$NOX.Out)
W = 0.9805, p-value = 0.8518

> shapiro.test(log(PineyPoll$Ortho.Ctrl))

        Shapiro-Wilk normality test

data:  log(PineyPoll$Ortho.Ctrl)
W = 0.9723, p-value = 0.6229

> shapiro.test(log(PineyPoll$Ortho.Out))

        Shapiro-Wilk normality test

data:  log(PineyPoll$Ortho.Out)
W = 0.9557, p-value = 0.2567

> shapiro.test(log(ON.Ctrl))

        Shapiro-Wilk normality test

data:  log(ON.Ctrl)
```

```
W = 0.902, p-value = 0.01096

> shapiro.test(log(ON.Out))

        Shapiro-Wilk normality test

data:  log(ON.Out)
W = 0.9705, p-value = 0.5721

> shapiro.test(log(PineyPoll$Cu.Ctrl))

        Shapiro-Wilk normality test

data:  log(PineyPoll$Cu.Ctrl)
W = 0.9475, p-value = 0.3574

> shapiro.test(log(PineyPoll$Cu.Out))

        Shapiro-Wilk normality test

data:  log(PineyPoll$Cu.Out)
W = 0.8385, p-value = 0.004383

> shapiro.test(log(PineyPoll$Pb.Ctrl))

        Shapiro-Wilk normality test

data:  log(PineyPoll$Pb.Ctrl)
W = 0.9602, p-value = 0.5766

> shapiro.test(log(PineyPoll$Pb.Out))
Error in shapiro.test(log(PineyPoll$Pb.Out)) :
  all 'x' values are identical
> shapiro.test(log(PineyPoll$Zn.Ctrl))

        Shapiro-Wilk normality test

data:  log(PineyPoll$Zn.Ctrl)
W = 0.9428, p-value = 0.296

> shapiro.test(log(PineyPoll$Zn.Out))

        Shapiro-Wilk normality test

data:  log(PineyPoll$Zn.Out)
W = 0.2439, p-value = 5.28e-09

> wilcox.exact(PineyPoll$TSS.Ctrl,PineyPoll$TSS.Out,paired=T)

        Exact Wilcoxon signed rank test

data:  PineyPoll$TSS.Ctrl and PineyPoll$TSS.Out
V = 406, p-value = 7.451e-09
alternative hypothesis: true mu is not equal to 0

> wilcox.exact(PineyPoll$TP.Ctrl,PineyPoll$TP.Out,paired=T)

        Exact Wilcoxon signed rank test

data:  PineyPoll$TP.Ctrl and PineyPoll$TP.Out
V = 406, p-value = 7.451e-09
alternative hypothesis: true mu is not equal to 0

> wilcox.exact(PineyPoll$Ortho.Ctrl,PineyPoll$Ortho.Out,paired=T)
```

```
        Exact Wilcoxon signed rank test

data:  PineyPoll$Ortho.Ctrl and PineyPoll$Ortho.Out
V = 435, p-value = 3.725e-09
alternative hypothesis: true mu is not equal to 0

> wilcox.exact(PineyPoll$TN.Ctrl,PineyPoll$TN.Out,paired=T)

        Exact Wilcoxon signed rank test

data:  PineyPoll$TN.Ctrl and PineyPoll$TN.Out
V = 432, p-value = 1.863e-08
alternative hypothesis: true mu is not equal to 0

> wilcox.exact(PineyPoll$NOX.Cntrl,PineyPoll$NOX.Out,paired=T)

        Exact Wilcoxon signed rank test

data:  PineyPoll$NOX.Cntrl and PineyPoll$NOX.Out
V = 0, p-value = 3.725e-09
alternative hypothesis: true mu is not equal to 0

> wilcox.exact(PineyPoll$NH3.Ctrl,PineyPoll$NH3.Out,paired=T)

        Exact Wilcoxon signed rank test

data:  PineyPoll$NH3.Ctrl and PineyPoll$NH3.Out
V = 369, p-value = 0.0006071
alternative hypothesis: true mu is not equal to 0

> wilcox.exact(PineyPoll$TKN.Ctrl,PineyPoll$TKN.Out,paired=T)

        Exact Wilcoxon signed rank test

data:  PineyPoll$TKN.Ctrl and PineyPoll$TKN.Out
V = 434, p-value = 7.451e-09
alternative hypothesis: true mu is not equal to 0

> wilcox.exact(ON.Ctrl,ON.Out,paired=T)

        Exact Wilcoxon signed rank test

data:  ON.Ctrl and ON.Out
V = 435, p-value = 3.725e-09
alternative hypothesis: true mu is not equal to 0

> wilcox.exact(PineyPoll$Cu.Ctrl,PineyPoll$Cu.Out,paired=T)

        Exact Wilcoxon signed rank test

data:  PineyPoll$Cu.Ctrl and PineyPoll$Cu.Out
V = 190, p-value = 3.815e-06
alternative hypothesis: true mu is not equal to 0

> wilcox.exact(PineyPoll$Pb.Ctrl,PineyPoll$Pb.Out,paired=T)

        Exact Wilcoxon signed rank test

data:  PineyPoll$Pb.Ctrl and PineyPoll$Pb.Out
V = 190, p-value = 3.815e-06
alternative hypothesis: true mu is not equal to 0

> wilcox.exact(PineyPoll$Zn.Ctrl,PineyPoll$Zn.Out,paired=T)
```

```
        Exact Wilcoxon signed rank test

data:  PineyPoll$Zn.Ctrl and PineyPoll$Zn.Out
V = 190, p-value = 3.815e-06
alternative hypothesis: true mu is not equal to 0
```